

Theoretical Study on the Kinetics of the Reaction of C₂H with C₂H₂

V. Saheb^{a,*}, A. Amiri^b and M.R. Noorbala^b

^aDepartment of Chemistry, Shahid Bahonar University of Kerman, P. O. Box: 76169-14111, Kerman, Iran

^bDepartment of Chemistry, Yazd University, P. O. Box: 89195-741, Yazd, Iran

(Received 21 July 2017, Accepted 16 October 2017)

In this theoretical research, the mechanism of the C₂H + C₂H₂ reaction is studied by high-level quantum-chemical methods, and kinetics of the reaction is investigated by statistical rate theories. High-level electronic structure calculation methods including M06-2X, CCSD(T), CBS-Q and G4 methods are employed to explore the doublet potential energy surface of the reaction and compute the molecular properties necessary for carrying out the statistical rate theory calculations. After locating stationary points of the reaction, steady-state approximation to the chemically-activated intermediates along with some statistical manipulations are applied to derive some practical integral equations for the rate constants of formation of all possible products of the reaction. Unimolecular rate constants are computed by RRKM theory. VRC-TST is used to compute the sum of quantum states for internal degrees of freedom of loose transition states. The present calculations reveal that the product HCCCCH + H (P8) is the dominant product over the whole pressure and temperature range considered in the present study. Nonetheless, at low temperatures and high pressures other intermediate products especially HCC(H)CCH and H₂CCCCH become significant. The overall computed rate constants are nearly constant over the temperature range 100-500 K and slightly increase at higher temperatures.

Keywords: Acetylene, Ethynyl radical, Kinetics, RRKM, VRC-TST

INTRODUCTION

The kinetics and mechanism of the reaction between ethynyl radical (C₂H) and acetylene (C₂H₂) have received considerable scrutiny due to its importance in combustion [1-8] and interstellar chemistry [9-11]. In hydrocarbon flames, the C₂H + C₂H₂ reaction is thought to be a key reaction for the subsequent formation of polyacetylenes (C_{2n}H₂), polycyclic aromatic hydrocarbons and soot [1-8]. In the initial stages of soot formation in hydrocarbon flames, more than 50% of the primary fuel is believed to pass via the formation of diacetylene (C₄H₂), the main product of the C₂H + C₂H₂ reaction [2,7]. The title reaction is an important neutral-neutral condensation process in interstellar space and planetary atmospheres leading to form more complex species [9-10].

To date, many researchers have used different apparatus to measure the pressure and temperature dependence of the kinetic parameters of the C₂H + C₂H₂ reaction [9-24]. A synopsis of these measured kinetic parameters are provided in Table 1. Although a temperature-independent value of about $1.5 \times 10^{-10} \text{ cm}^3 \text{ molecule}^{-1} \text{ s}^{-1}$ is determined by most of the research groups at temperatures around 298 K, higher values are reported by early measurements. The HCCCCH + H is known as the major product of the reaction. However, there are discordant data on the temperature dependence of the rate constants at lower and higher temperatures. There are reports in the literature on positive [15], and negative [21] and no temperature dependence [17] of the rate coefficients. In addition, no experimental and theoretical studies have been performed on the significance of other possible product channels of the title reaction.

There are two theoretical reports in the literature on the

*Corresponding author. E-mail: vahidsaheb@mail.uk.ac.ir

Table 1. The Arrhenius Parameters ($k = AT^n e^{-E_a/RT}$) for the Title Reaction Reported by Various Laboratories

T (K)	A ($\text{cm}^3 \text{ molecule}^{-1} \text{ s}^{-1}$)	n	E_a (kJ mol^{-1})	Ref. ^a
100-1500	4.63×10^{-12}	0.56	0.624	Present work
295-800	1.3×10^{-10}			Ceursters 2000 [24]
143-359	2.44×10^{-11}	1.8	-3.941	Opansky 1996 [22]
295-448	1.3×10^{-10}			van Look 1995 [21]
170-350	1.1×10^{-10}		-0.23	Pedersen 1993 [20]
295-854	1.6×10^{-10}			Farhat 1993 [19]
298-2177	1.50×10^{-10}			Koshi 1992 [18]
296-1475	3.02×10^{-10}		1.95	Shin 1991 [15]
298	1.51×10^{-10}			Stephens 1987 [16]
298	3.10×10^{-11}			Laufer 1979 [13]
320	4.98×10^{-11}			Lange 1975 [12]

^aThe values in the parentheses are the corresponding reference numbers.

title reaction [9]. Herbst and Woon have used a simple approach for computing the rate coefficient for the formation of HCCCCH + H. They have employed the phase-space approach on the base of a long-range potential which is assumed to be the sum of dispersion and induction terms. Ceursters *et al.* [24] have also investigated the PES of the $\text{C}_2\text{H} + \text{C}_2\text{H}_2$ reaction. They have optimized the structures of the stationary points at the B3LYP/6-311++G(d,p) level of theory and performed single-point calculations at the CCSD(T)/6-311++G(d,p) level. In this research, statistical rate theories are employed to compute the rate constants for all possible reaction channels. First, the potential energy surface (PES) of the $\text{C}_2\text{H} + \text{C}_2\text{H}_2$ reaction is explored to compute the structures and energies of the stationary points of the reaction. Next, transition state theory (TST) and RRKM statistical rate theories are used to compute the rate coefficients for different product channels at different temperatures and pressures. The obtained results

are compared with the available experimental and theoretical data.

COMPUTATIONAL DETAILS

Electronic-Structure Calculations

In the present research work, some well-tested electronic structure calculation methods are employed to optimize geometries and evaluate the energies of the stationary points on the PES of the title reaction. The geometries of the minimum energy structures and saddle points are fully optimized by the M06-2X hybrid *meta* density functional theory (HMDFT) method [25] along with the MG3S basis set [26]. The performance of the M06-2X method, developed by Truhlar and coworkers, is illustrated for representative databases containing energetic data, bond lengths, vibrational frequencies and vibrational zero point energies [25]. More accurate energies are obtained by

single-point energy calculations at the unrestricted coupled cluster method with single, double and noniterative triple excitations UCCSD(T) [27] in combination with the standard AugH-cc-pVTZ+2df basis set [28]. In the latter basis set, the augmented correlation-consistent polarized triple- ζ basis set Aug-cc-pVTZ [29] is extended by adding high exponent d- and f-type basis functions so that inner-shell correlation effects are more correctly described. All electrons are included in the correlation calculations. In addition, spin-restricted open-shell calculations at the ROCCSD(T)/AugH-cc-pVTZ+2df are also carried out which are discussed in the next sections.

Additional single-point calculations are carried out by the high-level combination methods CBS-Q [30] and G4 [31] on the optimized geometries at the M06-2X/MG3S level of theory for the purpose of comparison. In CBS-Q and G4 methods, energy is usually calculated as a combination of single-point calculations on the geometries optimized at the B3LYP level. However, it is proved that B3LYP method is not a suitable method for geometry optimization of transition states [32]. All of the quantum chemical calculations are carried out with the Gaussian 09 package of programs [33].

Dynamical Calculations

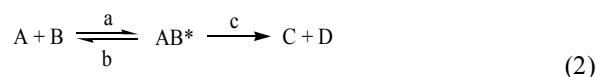
As it is discussed in detail in the next section, the reaction C₂H + C₂H₂ occurs via the addition of C₂H radical to the carbon of the triple bond of acetylene, leading to a primary chemically activated intermediate denoted as INT3. This intermediate may undergo unimolecular reactions to yield the reactants, other intermediates and products, or can be de-activated by molecular collisions. RRKM theory is usually used to compute the rate constants for decomposition of the vibrationally excited molecules [34-35]. According to the RRKM theory, the energy-dependent rate constant for a unimolecular reaction is given by the following equation:

$$k(E) = \sigma \frac{Q_1^+ G(E_v^+)}{Q_1 h \rho(E)} \quad (1)$$

where $G(E_v^+)$ is the sum of active vibrational and rotational states for the transition state, $\rho(E)$ is the density of active quantum states for reactant, Q_1^+ and Q_1 are the partition

functions for the adiabatic rotations in the transition state and reactant. In this research, Beyer-Swinehart direct count algorithm is used to compute $G(E_v^+)$ and $\rho(E)$ [36]. The values of $k(E)$, $\rho(E)$ and $G(E_v^+)$ are calculated by using RRKM program from Zhu and Hase [37]. Tunneling probabilities are accounted for by computing the transmission probability for an Eckart potential barrier [38].

When a chemically-activated intermediate is formed during the reaction of two species, transition state theory with the application of RRKM theory to the unimolecular decomposition of the chemically-activated intermediate could be used to compute the rate constants for a bimolecular reaction [39].



By applying steady-state approximation to the activated intermediate and performing some statistical mechanical manipulations, the following expression for the rate coefficient of disappearance of the reactants are derived [39]:

$$k = \frac{\sigma B_e}{h} \frac{q_{tr}^+}{q_A q_B} e^{-\frac{E_a}{RT}} \int_0^\infty \frac{(\omega + k_e) G(E_{vr}^+)}{(\omega + k_e + k_e')} e^{-\frac{E^+}{RT}} dt \quad (3)$$

In Eq. (3), k_e and k_e' are the energy-specific rate constants for unimolecular decomposition of the chemically-activated adduct to the reactants and products, respectively. q_A and q_B are the total partition functions for reactants A and B excluding electronic degrees of freedom while q_{tr}^{\ddagger} is the product of translational and rotational partition functions for the transition state of entrance channels. B_e is the quotient of electronic partition functions of transition state and reactants, and σ is the reaction path degeneracy. The de-energization rate constant for the activated adduct, ω , is given by

$$\omega = \beta_c Z_{coll} [M] \quad (4)$$

where β_c is the collision deactivation efficiency, Z_{coll} is the collision frequency and $[M]$ is the bath gas concentration. β_c corresponds to energy transferred in collisions according to

the following expression [40]:

$$\beta_c = \left(\frac{\langle \Delta E \rangle_{down}}{\langle \Delta E \rangle_{down} + F_E k_B T} \right)^2 \quad (5)$$

In the above equation, $\langle \Delta E \rangle_{down}$ is the average energy transferred in a deactivating collision and F_E is the energy dependence of the density of states. The values of $\langle \Delta E \rangle_{down}$ are not measured for many molecules including the intermediates formed in the $C_2H + C_2H_2$ reaction. In the absence of this experimental data, the reliable values for similar molecules could be used. The value of $\langle \Delta E \rangle_{down}$ for iso- C_3H_7 radical in N_2 bath gas have been determined by Pilling and coworkers [41] to be 129 cm^{-1} by analysis of the unimolecular rate constants in the fall-off region. The iso- C_3H_7 radical has similar structures to the activated intermediate radicals formed in the present study. Therefore, the value of 129 cm^{-1} is adopted here for computing the collision deactivation efficiencies.

When a reaction proceeds through many activated adducts, similar equations as Eq. (3) could be derived [42-44]. By applying steady-state approximation to the activated intermediates and performing similar statistical mechanics manipulations, expressions for the rate constants of individual channels are obtained. By a similar procedure, expressions for different possible products originating from $C_2H + C_2H_2$ reaction are obtained which are discussed in the next section.

One important feature of the title reaction is that the entrance channel forming the initial activated intermediate, $HC_2-CH=CH_2$, is a barrierless process. In the case of an association process which proceeds through a not well-defined saddle-point, special theories should be used to estimate the sum of states of transition state. Here, there is a loose transition state in which some internal degrees of freedom have become complicated hindered internal rotations. In VRC-TST, these internal motions are called "transitional modes" [45-50]. The other vibrational modes whose natures do not change significantly during the process are called "conserved" modes. Next, the sum of states is computed according to the following convolution:

$$N_{EJ} = \int_0^{E'} N_V(E' - \epsilon) \Omega_J(\epsilon) d\epsilon \quad (6)$$

In the above equation, $\Omega_J(\epsilon)d\epsilon$ is the number of states for the transitional modes within the energy element $(\epsilon, \epsilon + d\epsilon)$ at the given J . $N_V(E' - \epsilon)$ is the number of quantum states for the conserved vibrational modes with energy less than or equal to $E' - \epsilon$ where E' is the available energy of the transition state, *i.e.* E minus the potential energy minimum, $V(s)$, at the given value of the reaction coordinate. The number of states in transitional modes should be evaluated by classical statistical mechanical methods. Here, $\Omega_J(\epsilon)d\epsilon$ is computed by Monte Carlo integration of the phase space volume. The conserved modes are treated quantum mechanically. In order to compute the phase space volume for the transitional modes, it is necessary to have a potential energy function for the interaction between separating fragments. Klippenstein *et al.* have assumed that the potential energy function for transitional modes is the sum of a bonding potential for the breaking (or associating) bond and a non-bonded potential for the other inter-fragment interactions [48-50].

$$V = V_B + V_{NB} \quad (7)$$

The bonding part of the potential is considered as a Morse or Varshni potential multiplied by an orientation factor representing the angular dependence of bonding energy.

$$V_B = V_V(R) \cos^2(\theta_1 - \theta_{1,e}) \cos^2(\theta_2 - \theta_{2,e}) \quad (8)$$

In Eq. (8), θ_1 and θ_2 are the angles between bonding axis connecting two fragments and reference axes in the separating fragments, where $\theta_{1,e}$ and $\theta_{2,e}$ are the equilibrium values of θ_1 and θ_2 . The Varshni potential is used in the present study which is given by following expression:

$$V_V(R) = D \left\{ 1 - \left(\frac{r_e}{r} \right) \exp[-\beta(r^2 - r_e^2)] \right\}^2 - D \quad (9)$$

where D is bonding energy, r_e is the equilibrium bonding distance and β is a parameter that controls the shape of the potential energy curve. The non-bonding potential is taken as a sum of 6-12 Lennard-Jones potentials between the non-bonded atoms of the two fragments.

$$V_{NB} = \sum_{i,j} 4 \epsilon_{ij} \left[\left(\frac{\sigma_{ij}}{r_{ij}} \right)^{12} - \left(\frac{\sigma_{ij}}{r_{ij}} \right)^6 \right] \quad (10)$$

In Eq. (10), the parameters σ_{ij} and ϵ_{ij} are the usual Lennard-Jones parameters for the van der Waals interaction between atoms i and j ; r_{ij} is the separation distance between atoms i and j . The prime indicates that the bond atoms are not included in the sum. Variflex code [51] developed by Klippenstein and coworkers is used to perform VRC-TST calculations.

RESULTS AND DISCUSSION

As aforementioned, Ceursters et al. [24] have also explored the PES of the C₂H + C₂H₂ reaction at the CCSD(T)/6-311++G(d,p) level of theory. In the present study, higher levels of theory is employed to optimize the structures of the intermediates, transition states and products of the reaction and calculate their relative energies. On the basis of the geometries optimized at the M06-2X/MG3S level of theory, the mechanism of the reaction C₂H radical and acetylene can be demonstrated by Scheme 1. The z-matrices for reactants, intermediates and transition states arising from the C₂H + C₂H₂ reaction are given in Supplemental Information. The relative energies of the stationary points located on the doublet potential energy surface of the C₂H + C₂H₂ reaction computed at M06-2X/MG3S, CBS-Q, G4, UCCSD(T)/Aug-cc-pVTZ+2df and ROCCSD(T)/Aug-cc-pVTZ+2df levels of theory are listed in Table 2. As it is seen, the computed energies are slightly dependent on the employed quantum-chemical methods. In addition, due to the presence of two multiple bond systems, the wave functions are spin-contaminated with large expectation values for $\langle S^2 \rangle > 1.0$. The latter points about the title reaction have also been mentioned by Ceursters *et al.* [24]. A recent research shows that one should be very careful using spin-unrestricted methods with high values of $\langle S^2 \rangle$ [52]. Blanquart has obtained a good set of estimates for the enthalpies of formation for some critical polycyclic aromatic hydrocarbon radicals using spin-restricted open-shell ROCCSD(T) calculations [52].

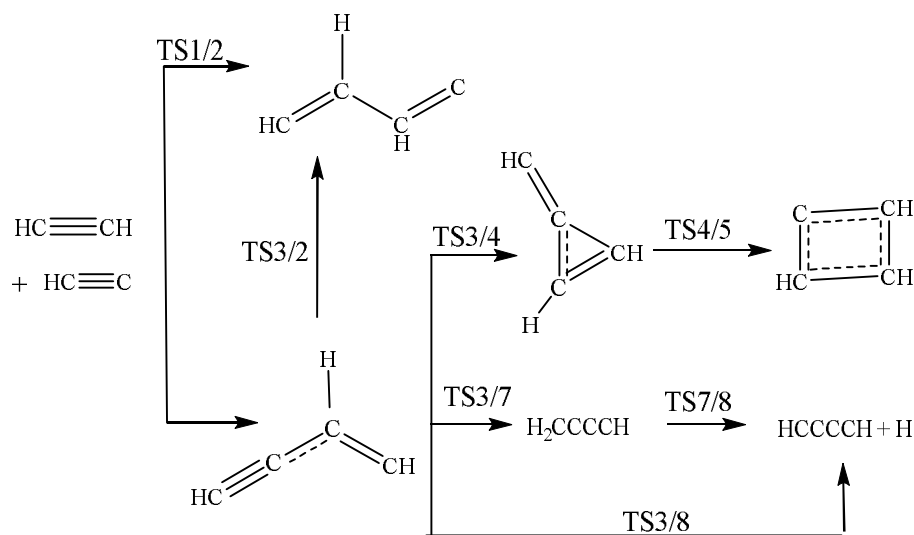
The highest levels of theory used in the present research are UCCSD(T)/Aug-cc-pVTZ+2df and ROCCSD(T)/Aug-

cc-pVTZ+2df. As can be seen from Table 2, there is a good agreement between the computed energies (at least for kinetically important species) at these two levels. Considering the points mentioned above, the computed energies at the ROCCSD(T)/Aug-cc-pVTZ+2df are used to perform kinetic calculations. The potential energy profile of the reaction at the ROCCSD(T) level of theory is depicted in Fig. 1.

The reaction proceeds via the addition of each carbon atom of C₂H radical to either of the carbon atom of the triple bond of HC≡CH, leading to the product P2 or the intermediate INT3. According to the energies computed at the ROCCSD(T)/Aug-cc-pVTZ+2df level, the barrier height for the formation of P2 *via* TS1/2 is 18.7 kJ mol⁻¹. P2, in which C₂H is attached via its central carbon atom to the carbon atom of acetylene, is 70.4 kJ mol⁻¹ more stable than the reactants. As mentioned in the previous section, the formation of INT3 is a barrierless process; *i.e.*, no well-distinguished saddle-point is formed during the process. The energy of INT3 is 264.3 kJ mol⁻¹ lower than the reactants. Next, INT3 isomerizes to give the three member ring intermediate INT4 by passing through the transition state TS3/4. The barrier height for this process is 108.3 kJ mol⁻¹ and the energy of INT4 is 87.0 kJ mol⁻¹ higher than INT3. INT4 may in turn undergo an isomerization reaction to give four-membered ring P5. The barrier height of the latter isomerization reaction from INT4 is 139.9 kJ mol⁻¹ and energy of P5 is 18.1 kJ mol⁻¹ higher than that for INT4.

INT3 may be also converted to P2 *via* TS3/2 with the barrier height of 183.6 J mol⁻¹. INT3 passes through the transition state TS3/7 with the barrier height of 171.7 kJ mol⁻¹ to give the intermediate INT7. The energy of INT7 is 55.1 kJ mol⁻¹ lower than INT3. INT7 is decomposed to yield HCCCCH + H (P8) via the transition state TS7/8 with an energy of 191.7 kJ mol⁻¹ higher than INT7. The intermediate INT3 can be also directly decomposed to P8 through the transition state TS3/8. The barrier height of this process is 154.5 kJ mol⁻¹.

The harmonic vibrational frequencies and the principle moments of inertia of the reactants, intermediates and transition states used in kinetic calculations, calculated at the M06-2X/MG3S level of theory, are provided in Table 2S in Supplemental Information. A careful look at the PES of the reaction shows that the formation of P2 is not



Scheme 1

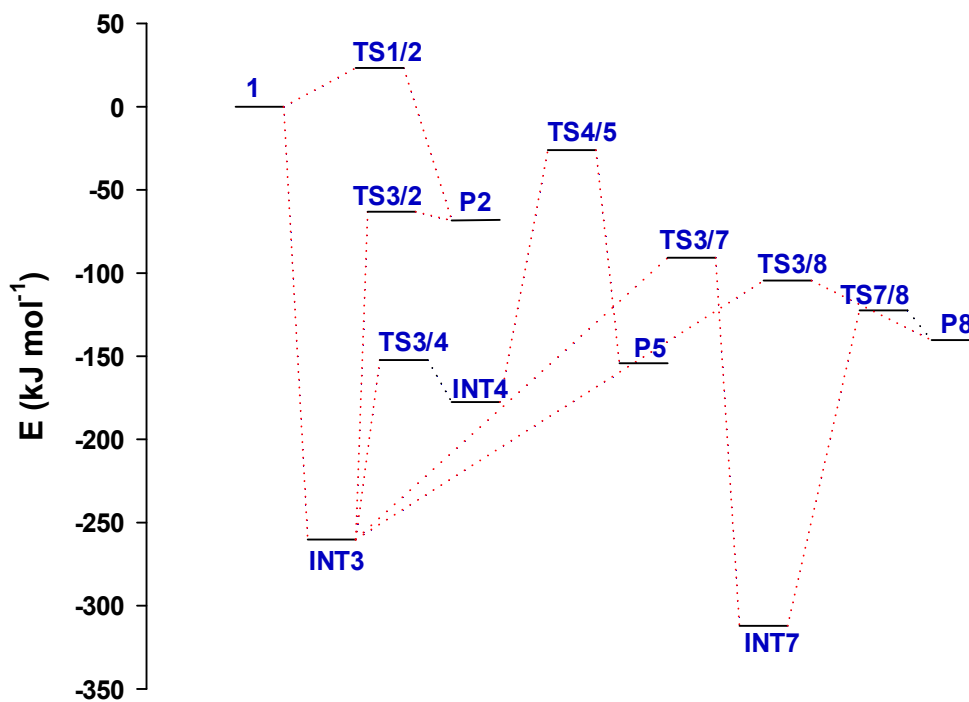


Fig. 1. Relative energies of the stationary points located on the doublet ground-state potential energy surface of the reaction $C_2H + C_2H_2$. The energy values are given in kJ mol^{-1} and are calculated at the CCSD(T,full)/AugH-cc-pVTZ+2df theory.

Table 2. The Relative Energies of the Stationary Points for the C₂H + C₂H₂ Reaction Computed at some Levels of Theory in kJ mol⁻¹. All Values are Corrected for Zero Point Energies

	CBS-QB3	G4	M06-2X ^a	UCCSD(T) ^b	ROCCSD(T) ^b	CCSD(T) ^c
P2	-51.1	-48.2	-53.6	-68.4	-70.4	-55
INT3	-246.5	-243.6	-251.8	-260.2	-264.3	-239
INT4	-157.6	-155.8	-184.6	-177.5	-177.3	-147
P5	-139.7	-137.2	-144.7	-154.2	-159.2	-130
INT7	-299.4	-289.0	-304.8	-312.1	-319.4	-295
P8	-117.4	-113.4	-123.5	-140.3	-140.3	-110
TS1/2	35.9	40.4	26.6	23.3	18.7	32
TS3/4	-137.9	-132.2	-144.1	-152.3	156.0	-123
TS3/2	-53.1		-69.1	-73.1	-80.7	
TS3/7			-80.1	-90.7	-92.6	-65
TS3/8	-91.8	-86.9	-88.8	-104.5	-109.8	-73
TS4/5	-12.3	-11.3	-26.5	-26.0	-37.4	
TS7/8	-106.2	-103.5	-107.9	-122.4	-127.7	-98

^aThe basis set MG3S is used. ^bThe basis set AugH-cc-pVTZ+2df is used. ^cThe basis set 6-311++G** is used (Ref. [24]).

kinetically feasible. The barrier height for the formation of P2 from reactants is relatively higher than the barrier-less process of formation of INT3. Although P2 is also formed from INT3, but the barrier height for the decomposition of P2 back to INT3 is negligible, so that it will be decomposed before it is deactivated by collisions. Therefore, in this research, it is mainly concentrated on the reaction path passing through INT3. By applying steady-state approximation to the intermediates INT3, INT4, INT5 and INT7, and performing some statistical mechanical manipulations [42-44], the following expressions for the rate constants of various products are obtained.

$$k_{INT3} = \frac{\sigma B_e q_{tr}^+}{h q_A q_B} e^{-\frac{E_a}{RT}} \int_0^\infty \frac{\omega G(E_{vr}^+)}{B1} e^{-\frac{E^+}{RT}} dE^+ \quad (11)$$

$$k_{INT4} = \frac{\sigma B_e q_{tr}^+}{h q_A q_B} e^{-\frac{E_a}{RT}} \int_0^\infty \frac{\omega k_{34} G(E_{vr}^+)}{B1 \times B2} e^{-\frac{E^+}{RT}} dE^+ \quad (12)$$

$$k_{INT5} = \frac{\sigma B_e q_{tr}^+}{h q_A q_B} e^{-\frac{E_a}{RT}} \int_0^\infty \frac{\omega k_{45} k_{34} G(E_{vr}^+)}{B1 \times B2 \times B3} e^{-\frac{E^+}{RT}} dE^+ \quad (13)$$

$$k_{INT7} = \frac{\sigma B_e q_{tr}^+}{h q_A q_B} e^{-\frac{E_a}{RT}} \int_0^\infty \frac{\omega k_{37} G(E_{vr}^+)}{B1 \times B4} e^{-\frac{E^+}{RT}} dE^+ \quad (14)$$

$$k_{INT8} = \frac{\sigma B_e q_{tr}^+}{h q_A q_B} e^{-\frac{E_a}{RT}} \int_0^\infty \left(\frac{k_{78} k_{37}}{B4} + k_{38} \right) \frac{G(E_{vr}^+)}{B1} e^{-\frac{E^+}{RT}} dE^+ \quad (15)$$

B1 to B4 in the above integrals are obtained from the following expressions:

$$B1 = k_{37} + k_{38} + k_{34} + k_{31} + \omega \quad (16)$$

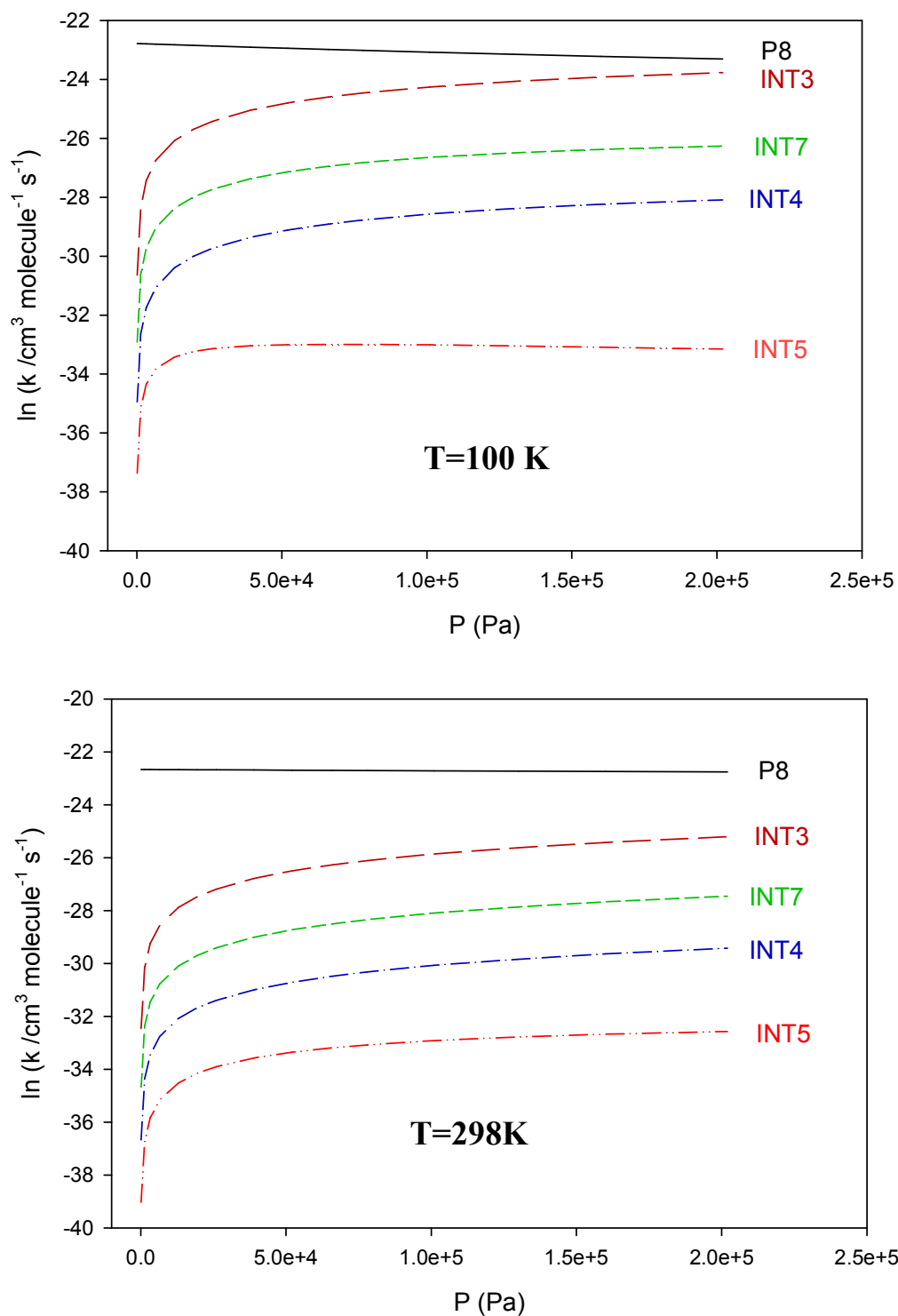


Fig. 2. The thermal rate coefficients for the important product channels computed at temperatures 100, 298 and 1000 K as a function of bath-gas pressure.

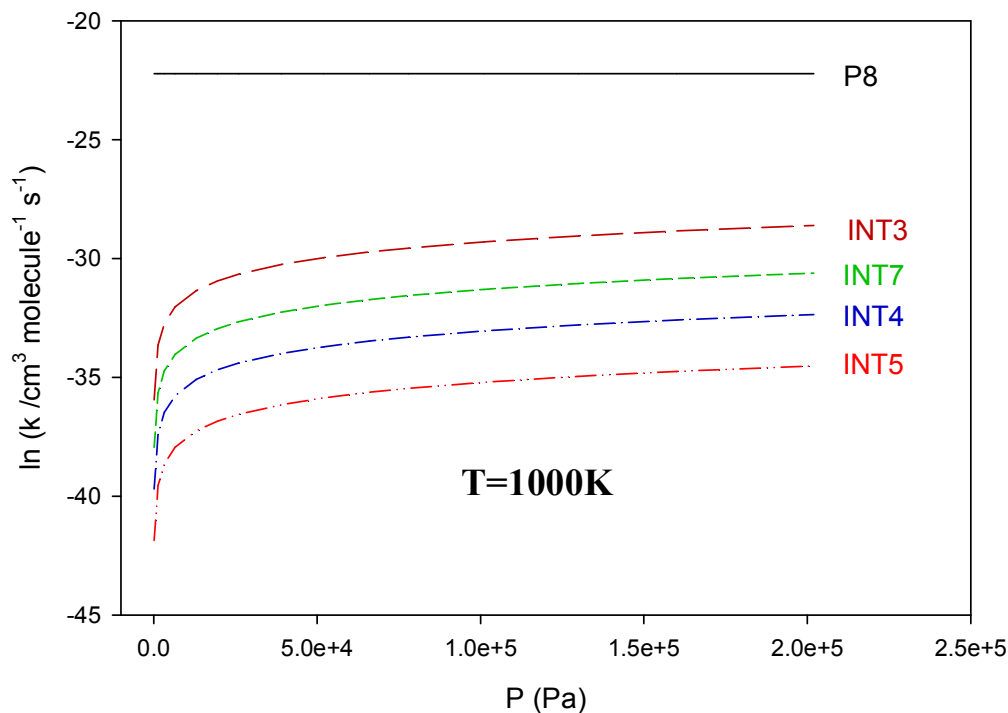


Fig. 2. Continued.

$$B2 = k_{43} + k_{45} + \omega - \frac{k_{45} k_{54}}{k_{54} + \omega} \quad (17)$$

$$B3 = k_{54} + \omega \quad (18)$$

$$B4 = k_{73} + k_{78} + \omega \quad (19)$$

In the above equations, k_{ij} is the microcanonical rate constant for the conversion of the intermediate i to the intermediate or product j . Other quantities are defined as Eq. (3). The derivation of the formula 11 to 19 are given in Supplemental information. The RRKM theory (Eq. (1)) is employed to compute the rate constants at many energies. Regarding the entrance channel, Eq. (6) is used to compute sum of quantum states. In order to compute the sum of quantum states, the distance between carbon atoms in two species C₂H and C₂H₂ are considered as reaction coordinate. It is worthy to mention here that the position of bottleneck (the structure with minimum sum of states) moves to smaller C-C bond distances as molecular energy increases. This is in accordance with previous calculations

reported in the literature [50]. In order to compute the integrals in the Eqs. (11) to (19) numerically, the energy-specific rate constants are computed with a step size $\Delta E^+ = 0.4 \text{ kJ mol}^{-1}$ up to 400 kJ mol^{-1} .

The calculated thermal rate coefficients at temperatures 100 K, 298 K and 1000 K for all important product channels, as a function of pressure, are demonstrated in Fig. 2. Our calculations reveal that the dominant product channel at all temperatures and pressures is HCCCCH + H (P8) and other products have smaller contributions to the overall rate coefficient. This is a reasonable result because the barrier height for the decomposition of the initially formed energized intermediate INT3 to the product P8 is much lower than that for its dissociation back to the reactants (C₂H + C₂H₂). In addition, INT3 also isomerizes to INT7 which is in turn decomposed finally to P8. It is noteworthy to mention that the unimolecular rate coefficient at a specified energy usually decreases with increasing internal degrees of freedom of a molecule. Here, the energized adducts INT3 and INT7 are relatively small molecules and their energy-specific rate coefficients is much higher than

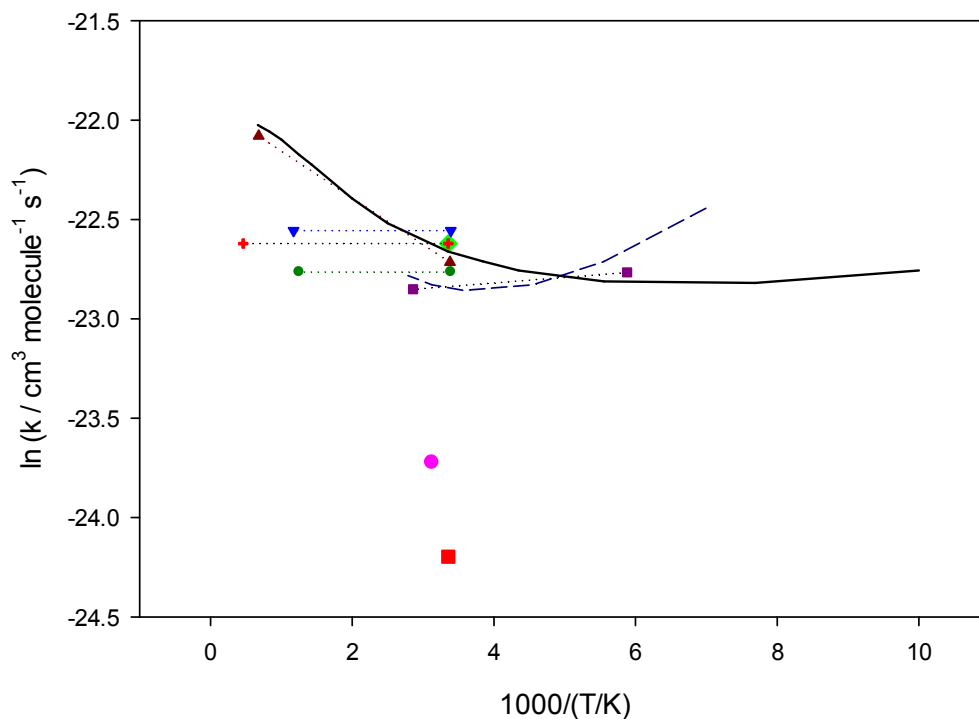


Fig. 3. The thermal overall rate coefficients for the $C_2H + C_2H_2$ reaction computed at temperatures in the range of 100-2000 K. “Solid line” is calculated data. Experimental data are given for the purpose of comparison. (●) from Ref. [12], (▼) from Ref. [19], (■) from Ref. [13], (▲) from Ref. [15], (◆) from Ref. [16], (+) from Ref. [17], (■) from Ref. [20], “dashed line” from Ref. [22], (●) from Ref. [24].

their de-energization rate constants. As a consequence, the product P8 is dominant channel and nearly pressure independent. As temperature decreases, the formation of the intermediates INT3, INT4, INT5 and INT7 become important. The reason is that at lower temperatures, the intermediates with lower internal energies are formed and consequently the deactivation processes become important. It should be mentioned that the rate constants for the formation of chemically-activated intermediates are pressure-dependent. This is a reasonable result because the rate constants for the de-activation of the active intermediates depend on the pressure of the system, see Eq. (4).

The computed overall rate coefficients are pressure independent since the rate coefficients for the dominant channel (channel P8) does not depend on the pressure. The temperature-dependence of the overall rate constants are depicted in Fig. 3 in comparison with the available

experimental data. The present overall computed rate constants are nearly constant over the temperature range 100-500 K and slightly increase at higher temperatures. The present theoretical results is in accordance with most of the experimental data. The empirical data of Refs. [12] and [13] are slightly lower than the other experimental data and present computed rate coefficients. The overall computed rate constants obtained in the present work are fitted to an extended Arrhenius equation. The values of parameters are reported in Table 1. In addition, the numerical calculated values of the rate coefficients along with the corresponding experimental values for some selected temperatures are provided in the Supplemental Information. As mentioned in the Introduction section, Herbst and Woon [9] have used a phase-space approach to compute the overall rate coefficient (being considered the HCCCCH + H as the only product of the reaction). Their computed rate coefficients are about a factor of 4 greater than the largest experimental values. As

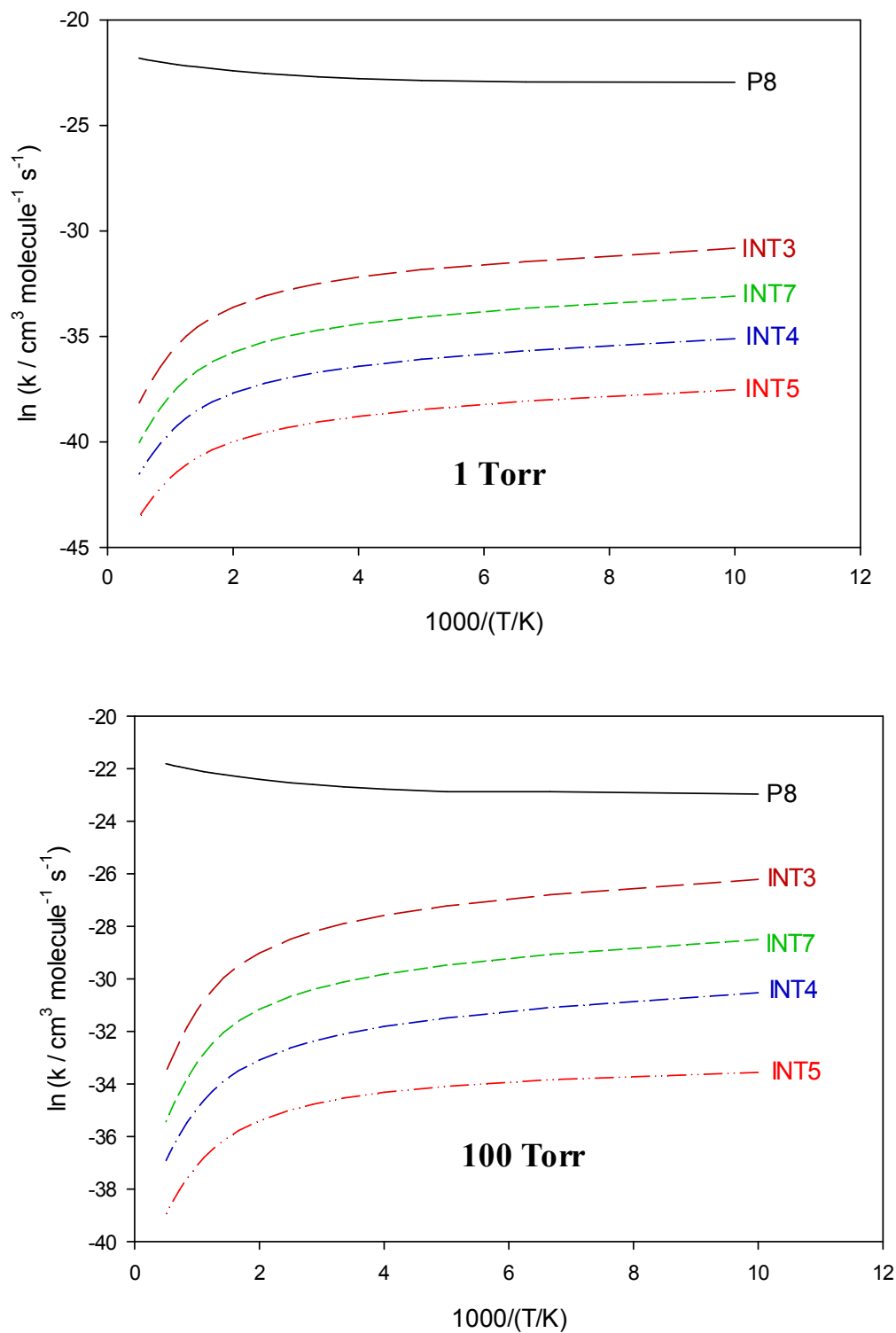


Fig. 4. The thermal rate coefficients for important product channels of the C₂H + C₂H₂ reaction computed at temperatures in the range of 100-2000 K and at the pressures 10, 100 and 760 Torr.

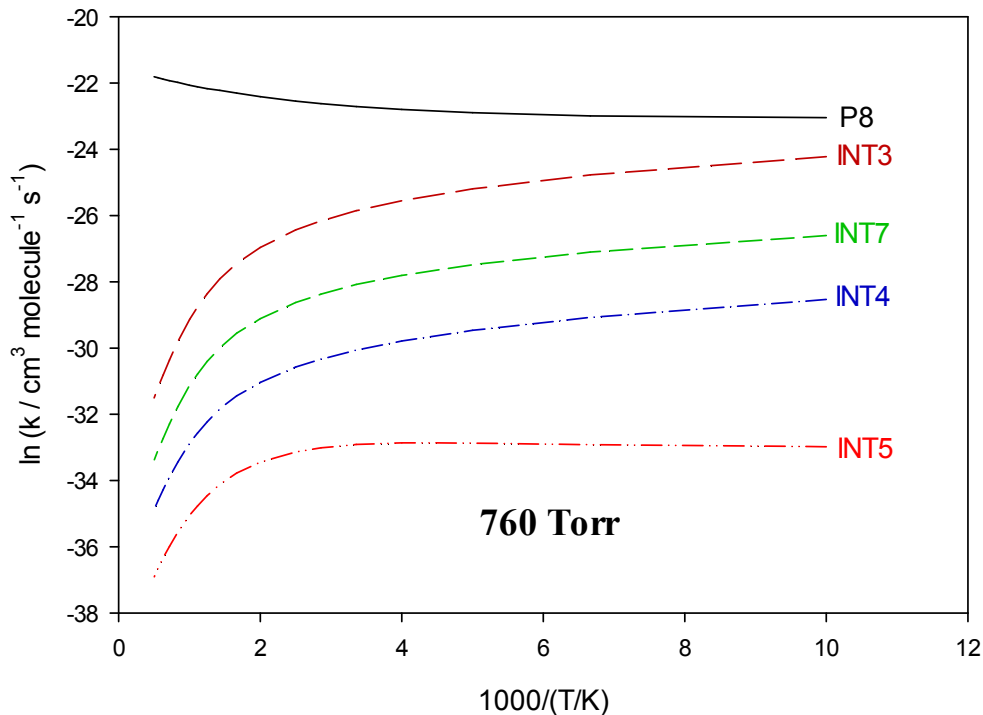


Fig. 4. Continued.

the authors have declared, their calculated rate coefficients are too large because the centrifugal barrier occurs at a sufficiently small distance (compared to the physical sizes of the two reactants) that the isotropic approximation is not justified.

The computed rate coefficients for the formation of various products as a function of temperature at the pressures 1, 100 and 760 Torr are plotted in Figs. 4. It is seen that the product channel P8 is the dominant product channel at all temperatures and pressures. However, as pressure increases, the rate constants for the formation of all intermediates increases due to increasing the rate of collisional deactivation processes. In the interstellar spaces where the temperature is very low, it is predicted that the intermediates such as HCC(H)CCH and H₂CCCCH become important.

CONCLUSIONS

In this research, the kinetics and mechanism of the

C₂H + C₂H₂ reaction is investigated theoretically. High level electronic structure theories are employed to locate the stationary points on the potential energy surface of the reaction and compute their rovibrational properties and energies. Statistical rate theories are employed to compute the rate constants of various possible products as a function of temperature and pressure. Our calculations reveal that the main reaction product at all temperatures and pressures is HCCCCH + H. Nonetheless, at high pressures (where the number of molecular collisions increases) and low temperatures (where low-energy intermediates are formed), the rate coefficients for the formation of HCC(H)CCH and HCCCCH₂ become important.

ACKNOWLEDGMENTS

The financial support of Shahid Bahonar University of Kerman is acknowledged.

REFERENCES

- [1] Bonne, U.; Homann, K. H.; Wagner, H. G., Carbon formation in premixed flames. *Symp. (Int.) Combust. [Proc.]*, **1965**, *10*, 503-512, DOI: 10.1016/S0082-0784(65)80197-7.
- [2] Warnatz, J., The mechanism of high temperature combustion of propane and butane. *Combust. Sci. Technol.*, **1983**, *34*, 177-200, DOI: 10.1080/00102208308923692.
- [3] Bittner, J. D.; Howard, J. B., Mechanism of hydrocarbon decay in fuel-rich secondary reaction zones. *Symp. (Int.) Combust. [Proc.]*, **1982**, *19*, 211-221, DOI: 10.1016/S0082-0784(82)80191-4.
- [4] Frenklach, M.; Wang, H., Detailed modeling of soot particle nucleation and growth. *Symp. (Int.) Combust. [Proc.]*, **1990**, *23*, 1559-1566, DOI: 10.1016/S0082-0784(06)80426-1.
- [5] Lindstedt, R. P.; Skevis, G., Chemistry of acetylene flames, *Combust. Sci. Technol.*, **1997**, *125*, 73-137, DOI: 10.1080/00102209708935656.
- [6] Doute, C.; Delfau, J. -L.; Vovelle, C., Reaction mechanism for aromatics formation in a low pressure, premixed acetylene-oxygen/argon flame. *Combust. Sci. Technol.*, **1994**, *103*, 153-173, DOI: 10.1080/00102209408907692.
- [7] Warnatz, J., Hydrocarbon oxidation at high temperatures. *Ber. Bunsenges. Phys. Chem.*, **1983**, *87*, 1008-1022, DOI: 10.1002/bbpc.19830871111.
- [8] Bockhorn, H.; Fetting, F.; Wenz, H. W., Investigation of the formation of high molecular hydrocarbons and soot in premixed hydrocarbon-oxygen flames. *Ber. Bunsenges. Phys. Chem.*, **1983**, *87*, 1067-1073, DOI: 10.1002/bbpc.19830871121.
- [9] Herbst, E.; Woon, D. E., The rate of the reaction between C₂H and C₂H₂ at interstellar temperatures. *Astrophys. J.*, **1997**, *489*, DOI: 109-112, 10.1086/304786.
- [10] Chastaing, D.; James, P. L.; Sims, I. R.; Smith, I. W. M., Neutral-neutral reactions at the temperatures of interstellar clouds Rate coefficients for reactions of C₂H radicals with O₂, C₂H₂, C₂H₄ and C₃H₆ down to 15 K. *Faraday Discuss.* **1998**, *109*, 165-181, DOI: 10.1039/A800495A.
- [11] Kovačs, T.; Blitz, M. A.; Seakins, P. W., H atom yields from the photolysis of acetylene and from the reaction of C₂H with H₂, C₂H₂ and C₂H₄. *J. Phys. Chem. A*, **2010**, *114*, 4735-4741, DOI: 10.1021/jp908285t.
- [12] Lange, W.; Wagner, H. G., Massenspektrometrische untersuchungen über erzeugung und reaktionen von C₂H-radikalen. *Ber. Bunsenges. Phys. Chem.*, **1975**, *79*, 165-170, DOI: 10.1002/bbpc.19750790210.
- [13] Laufer, A. H.; Bass, A. M., Photochemistry of acetylene. bimolecular rate constant for the formation of butadiyne and reactions of ethynyl radicals. *J. Phys. Chem.*, **1979**, *83*, 310-313, DOI: 10.1021/j100466a002.
- [14] Okabe, H., Photochemistry of acetylene at 1470 Å. *J. Chem. Phys.*, **1981**, *75*, 2772-2778, DOI: 10.1063/1.442348.
- [15] Shin, K. S.; Michael, J. V., Rate constants (296-1700 K) for the reactions C₂H + C₂H₂ = C₄H₂ + H and C₂D + C₂D₂ = C₄D₂ + D. *J. Phys. Chem.*, **1991**, *95*, 5864-5869, DOI: 10.1021/j100168a029.
- [16] Stephens, J. W.; Hall, J. L.; Solka, H.; Yan, W.-B.; Curl, R. F.; Glass, G. P., Rate constant measurements of reactions of C₂H with H₂, O₂, C₂H₂, and NO using color center laser kinetic spectroscopy. *J. Phys. Chem.*, **1987**, *91*, 5740-5743, DOI: 10.1021/j100306a044.
- [17] Koshi, M.; Fukuda, K.; Kamiya, K.; Matsui, H., Temperature dependence of the rate constants for the reactions of ethynyl radical with acetylene, hydrogen, and deuterium. *J. Phys. Chem.*, **1992**, *96*, 9839-9843, DOI: 10.1021/j100203a048.
- [18] Koshi, M.; Nishida, N.; Matsui, H., Kinetics of the reactions of C₂H with C₂H₂, H₂ and D₂. *J. Phys. Chem.*, **1992**, *96*, 5875-5880, DOI: 10.1021/j100193a043.
- [19] Farhat, S. K.; Morter, C. L.; Glass, G. P., Temperature dependence of the rate of reaction of C₂H with H₂. *J. Phys. Chem.*, **1993**, *97*, DOI: 12789-12792, 10.1021/j100151a026.
- [20] Pedersen, J. O. P.; Opansky, B. J.; Leone, S.R., Laboratory studies of low-temperature reactions of C₂H with C₂H₂ and implications for atmospheric models of titan. *J. Phys. Chem.*, **1993**, *97*, 6822-6829,

- DOI: 10.1021/j100128a013.
- [21] Van Look, H.; Peeters, J., Rate coefficients of the reactions of C₂H with O₂, C₂H₂, and H₂O between 295 and 450 K. *J. Phys. Chem.*, **1995**, *99*, 16284-16289, DOI: 10.1021/j100044a013.
- [22] Opansky, B. J.; Leone, S. R., Low-temperature rate coefficients of C₂H with CH₄ and CD₄ from 154 to 359 K. *J. Phys. Chem.*, **1996**, *100*, 4888-4892, DOI: 10.1021/jp9532677.
- [23] [23] Brachhold, H.; Alkemade, U.; Homann, K. H., Reactions of ethynyl radicals with alkynes in the system sodium vapour/ethynylbromide/alkyne. *Ber. Bunsenges. Phys. Chem.*, **1988**, *92*, 916-924, DOI: 10.1002/bbpc.198800220.
- [24] Ceursters, B.; Nguyen, H. M. T.; Peeters, J.; Nguyen, M. T., *Chem. Phys.*, **2000**, *262*, 243-252, DOI: 10.1016/S0301-0104(00)00337-2.
- [25] Zhao, Y.; Truhlar, D. G., The M06 suite of density functionals for main group thermochemistry, thermochemical kinetics, noncovalent interactions, excited states, and transition elements: two new functionals and systematic testing of four M06-class functionals and 12 other functional. *Theory Chem. Acc.*, **2008**, *120*, 215-241, DOI: 10.1007/s00214-007-0310-x.
- [26] Lynch, B. J.; Zhao, Y.; Truhlar, D. G., Effectiveness of diffuse basis functions for calculating relative energies by density functional theory. *J. Phys. Chem. A*, **2003**, *107*, 1384-1388, DOI: 10.1021/jp021590l.
- [27] Raghavachari, K.; Trucks, G. W.; Pople, J. A.; Head-Gordon, M., A fifth-order perturbation comparison of electron correlation theories. *Chem. Phys. Lett.*, **1989**, *157*, 479-483, DOI: 10.1016/S0009-2614(89)87395-6.
- [28] Martin, J. M. L.; de Oliveira, G., Towards standard methods for benchmark quality *ab initio* thermochemistry-W1 and W2 theory. *J. Chem. Phys.*, **1999**, *111*, 1843-1856, DOI: 10.1063/1.479454.
- [29] Kendall, R. A.; Dunning, T. H.; Harrison, R. J., Electron affinities of the first-row atoms revisited. Systematic basis sets and wave functions, Electron affinities of the first-row atoms revisited. *J. Chem. Phys.*, **1992**, *96*, 6796-6806, DOI: 10.1063/1.462569.
- [30] Montgomery Jr., J. A.; Frisch, M. J.; Ochterski, J. W.; Petersson, G. A., A complete basis set model chemistry. VI. Use of density functional geometries and frequencies. *J. Chem. Phys.*, **1999**, *110*, 2822-2827, DOI: 10.1063/1.477924.
- [31] Curtiss, L. A.; Redfern, P. C.; Raghavachari, K., Gaussian-4 theory. *J. Chem. Phys.*, **2007**, *126*, 084108:1-12, DOI: 10.1063/1.2436888.
- [32] Xu, X.; Alecu, I. M.; Truhlar, D. G., How well can modern density functionals predict internuclear distances at transition states? *J. Chem. Theory Comput.*, **2011**, *7*, 1667-1676, DOI: 10.1021/ct2001057.
- [33] Gaussian 09, Revision A.1, Frisch, M. J.; Trucks, G. W.; Schlegel, H. B.; Scuseria, G. E.; Robb, M. A.; Cheeseman, J. R.; Scalmani, G.; Barone, V.; Mennucci, B.; Petersson, G. A.; Nakatsuji, H.; Caricato, M.; Li, X.; Hratchian, H. P.; Izmaylov, A. F.; Bloino, J.; Zheng, G.; Sonnenberg, J. L.; Hada, M.; Ehara, M.; Toyota, K.; Fukuda, R.; Hasegawa, J.; Ishida, M.; Nakajima, T.; Honda, Y.; Kitao, O.; Nakai, H.; Vreven, T.; Montgomery, J. A., Jr.; Peralta, J. E.; Ogliaro, F.; Bearpark, M.; Heyd, J. J.; Brothers, E.; Kudin, K. N.; Staroverov, V. N.; Kobayashi, R.; Normand, J.; Raghavachari, K.; Rendell, A.; Burant, J. C.; Iyengar, S. S.; Tomasi, J.; Cossi, M.; Rega, N.; Millam, J. M.; Klene, M.; Knox, J. E.; Cross, J. B.; Bakken, V.; Adamo, C.; Jaramillo, J.; Gomperts, R.; Stratmann, R. E.; Yazyev, O.; Austin, A. J.; Cammi, R.; Pomelli, C.; Ochterski, J. W.; Martin, R. L.; Morokuma, K.; Zakrzewski, V. G.; Voth, G. A.; Salvador, P.; Dannenberg, J. J.; Dapprich, S.; Daniels, A. D.; Farkas, Ö.; Foresman, J. B.; Ortiz, J. V.; Cioslowski, J.; Fox, D. J. Gaussian, Inc., Wallingford CT, 2009.
- [34] Holbrook, K. A.; Pilling, M. J.; Robertson, S. H., Unimolecular Reactions. Wiley, Chichester, 1996.
- [35] Gilbert, R. G.; Smith, S. C., Theory of Unimolecular and Recombination Reactions. Blackwell Scientific, Oxford, 1990.
- [36] Beyer, T.; Swinehart, D. F., Algorithm 448: number of multiply-restricted partitions. *Assoc. Comput. Machines*, **1973**, *16*, 379, DOI: 10.1145/362248.362275.
- [37] Zhu, L.; Hase, W. L., QCPE Program 644, Quantum Chemistry Program Exchange. Indiana University,

Bloomington In.: 1993.

- [38] Johnston, H., Gas Phase Reaction Rate Theory. New York, Ronald, 1966.
- [39] Berman, M. R.; Lin, M. C., Kinetics and mechanism of the methylidyne + molecular nitrogen reaction. Temperature- and pressure-dependence studies and transition-state-theory analysis. *J. Phys. Chem.*, **1983**, *87*, 3933-3942, DOI: 10.1021/j100243a028.
- [40] Troe, J., Theory of thermal unimolecular reactions at low pressures. I. solutions of the master equation. *J. Chem. Phys.*, **1977**, *66*, 4745-4757, DOI: 10.1063/1.433837.
- [41] Seakins, P. W.; Robertson, S. H.; Pilling, M. J.; Slagle, I. R.; Gmurczyk, G.W.; Bencsura, A.; Gutman, D.; Tsang, W., Kinetics of the unimolecular decomposition of isopropyl: weak collision effects in helium, argon, and nitrogen. *J. Phys. Chem.*, **1993**, *97*, 4450-4458, DOI: 10.1021/j100119a032.
- [42] Hou, H.; Wang, B.; Gu, Y., *Ab initio* mechanism and multichannel RRKM-TST rate constant for the reaction of Cl(2P) with CH₂CO (Ketene). *J. Phys. Chem. A*, **2000**, *104*, 320-328, DOI: 10.1021/jp992829+.
- [43] Zhang, Y.; Sun, J.; Chao, K.; Sun, H.; Wang, F.; Tang, S. W.; Pan, X.; Zhang, J.; Wang, R., Mechanistic and kinetic study of CF₃CH=CH₂ + OH reaction. *J. Phys. Chem. A*, **2012**, *116*, 3172-3181, DOI: 10.1021/jp209960c.
- [44] Saheb, V., Theoretical studies on the kinetics of hydrogen abstraction reactions of H and CH₃ radicals from CH₃OCH₃ and some of their H/D isotopologues. *J. Phys. Chem. A*, **2015**, *119*, 4711-4717, DOI: 10.1021/acs.jpca.5b00911.
- [45] Klippenstein, S. J.; Implementation of RRKM theory for highly flexible transition states with a bond length as the reaction coordinate. *Chem. Phys. Lett.*, **1990**, *170*, 71-77, DOI: 10.1016/0009-2614(90)87092-6.
- [46] Klippenstein, S. J., An efficient procedure for evaluating the number of available states within a variably defined reaction coordinate framework. *J. Phys. Chem.*, **1994**, *98*, 11459-11464, DOI: 10.1021/j100095a032.
- [47] Wardlaw, D. M.; Marcus, R. A., Unimolecular reaction rate theory for transition states of any looseness. 3. application to methyl radical recombination. *J. Phys. Chem.*, **1986**, *90*, 5383-5393, DOI: 10.1021/j100412a098.
- [48] Wardlaw, D. M.; Marcus, R. A., RRKM reaction rate theory for transition states of any looseness. *Chem. Phys. Lett.*, **1984**, *110*, 230-234, DOI: 10.1016/0009-2614(84)85219-7.
- [49] Klippenstein, S. J.; Khundkar, L. R.; Zewail, A. H.; Marcus, R. A., Application of unimolecular reaction rate theory for highly flexible transition states to the dissociation of NCNO into NC and NO. *J. Chem. Phys.*, **1988**, *89*, 4761-4770, DOI: 10.1063/1.455670.
- [50] Klippenstein, S. J., A bond length reaction coordinate for unimolecular reactions. II. Microcanonical and canonical implementations with application to the dissociation of NCNO. *J. Chem. Phys.*, **1991**, *94*, 6469-6482, DOI: 10.1063/1.460276.
- [51] Klippenstein, S. J.; Wagner, A. F.; Dunbar, R. C.; Wardlaw, D. M.; Robertson, S. H., VARIFLEX: VERSION. 1.00, 1999.
- [52] Blanquart, G., Effects of spin contamination on estimating bond dissociation energies of polycyclic aromatic hydrocarbons. *Inter. J. Quantum Chemistry* **2015**, *115*, 796-801, DOI: 10.1002/qua.24904.